



# STRONG $\text{Ly}\alpha$ EMISSION IN THE PROXIMATE DAMPED $\text{Ly}\alpha$ ABSORPTION TROUGH TOWARD THE QUASAR SDSS J095253.83+011422.0

PENG JIANG<sup>1,2,3,4</sup>, HONGYAN ZHOU<sup>3,4</sup>, XIANG PAN<sup>3,4</sup>, NING JIANG<sup>4</sup>, XINWEN SHU<sup>5</sup>, HUIYUAN WANG<sup>4</sup>, QIUSHENG GU<sup>1,2</sup>, ZHENZHEN LI<sup>3,4</sup>, MAOCHUN WU<sup>4</sup>, XIHENG SHI<sup>3,4</sup>, TUO JI<sup>3,4</sup>, QIGUO TIAN<sup>3,4</sup>, AND SHAOHUA ZHANG<sup>3,4</sup>

<sup>1</sup>School of Astronomy and Space Science, Nanjing University, Nanjing, Jiangsu, 210093, China

<sup>2</sup>Key Laboratory of Modern Astronomy and Astrophysics (Nanjing University), Ministry of Education, Nanjing, Jiangsu, 210093, China

<sup>3</sup>Polar Research Institute of China, Jinqiao Road 451, Shanghai, 200136, China; zhouhongyan@pric.org.cn

<sup>4</sup>Key Laboratory for Research in Galaxies and Cosmology, The University of Science and Technology of China, Chinese Academy of Sciences, Hefei, Anhui, 230026, China

<sup>5</sup>Department of Physics, Anhui Normal University, Wuhu, Anhui, 241000, China

Received 2015 July 26; accepted 2016 February 8; published 2016 March 31

## ABSTRACT

SDSS J095253.83+011422.0 (J0952+0114) was reported by Hall et al. as an exotic quasar at  $z_{\text{em}} = 3.020$ . In contrast to prominent broad metal-line emission with  $\text{FWHM} \sim 9000 \text{ km s}^{-1}$ , only a narrow  $\text{Ly}\alpha$  emission line is present with  $\text{FWHM} \sim 1000 \text{ km s}^{-1}$ . The absence of a broad  $\text{Ly}\alpha$  emission line has been a mystery for more than a decade. In this paper, we demonstrate that this absence is due to dark proximate damped  $\text{Ly}\alpha$  absorption (PDLA) at  $z_{\text{abs}} = 3.010$  by identifying associated Lyman absorption line series from the damped  $\text{Ly}\beta$  up to  $\text{Ly}9$ , as well as the Lyman limit absorption edge. The PDLA cloud has a column density of  $\log N_{\text{H I}}(\text{cm}^{-2}) = 21.8 \pm 0.2$ , a metallicity of  $[\text{Zn}/\text{H}] > -1.0$ , and a spatial extent exceeding the narrow emission line region (NELR) of the quasar. With a luminosity of  $L_{\text{Ly}\alpha} \sim 10^{45} \text{ erg s}^{-1}$ , the residual  $\text{Ly}\alpha$  emission superposed on the PDLA trough is two orders of magnitude stronger than found by previous reports. This is best explained as re-radiated photons arising from the quasar outflowing gas on a larger scale than in the NELR. The PDLA here, acting like a natural coronagraph, provides us with valuable insight into the illuminated gases in the vicinity of the quasar, which are usually hard to resolve due to their small size and the “seeing fuzz” of bright quasars. Notably, J0952+0114 analogs might be easily omitted in the spectroscopic surveys of DLAs and PDLAs because their damped  $\text{Ly}\alpha$  troughs can be fully filled by additional strong  $\text{Ly}\alpha$  emissions. Our preliminary survey shows that such systems are not very rare. They could potentially be a unique sample for probing strong quasar feedback phenomena in the early universe.

*Key words:* quasars: absorption lines – quasars: emission lines – quasars: individual (SDSS J095253.83+011422.0)

## 1. INTRODUCTION

Damped  $\text{Ly}\alpha$  absorption systems (DLAs; reviewed in Wolfe et al. 2005) with a high neutral hydrogen column density are usually considered to be the main gas reservoir of star formation in the high-redshift universe (e.g., Wolfe et al. 1986; Nagamine et al. 2004; Prochaska et al. 2005). Since the emission of the background quasar is completely absorbed in the DLA trough, it has been proposed that the  $\text{Ly}\alpha$  emission from star formation in the DLA host galaxy can be observed with assistance from the natural coronagraph. However, most searches for residual  $\text{Ly}\alpha$  emission in the broad DLA trough of quasar spectra have resulted in non-detections (e.g., Smith et al. 1989; Kulkarni et al. 2006; Cai et al. 2014). Individual detections were sparsely reported, e.g., in the super-DLA with  $N_{\text{H I}} \approx 10^{22.1} \text{ cm}^{-2}$  toward Q1135-0010 (Kulkarni et al. 2012; Noterdaeme et al. 2012a), in the strong DLA with  $N_{\text{H I}} \approx 10^{21.6} \text{ cm}^{-2}$  toward PKS 0458-02 (Møller et al. 2004), and in the metal-rich DLA toward Q2222-0946 (Fynbo et al. 2010). Recently, Noterdaeme et al. (2014) studied a large sample of extremely strong DLAs (ESDLAs;  $N_{\text{H I}} \geq 10^{21.7} \text{ cm}^{-2}$ ) observed in the Baryon Oscillation Spectroscopic Survey (BOSS) of SDSS-III<sup>6</sup> and found significant residual  $\text{Ly}\alpha$  emission in the composite ESDLA

spectrum. The ESDLAs could plausibly be associated with galaxies that have high star formation rates (SFRs).

$\text{Ly}\alpha$  “blobs” have occasionally been discovered at close redshifts to quasars with tiny impact parameters of  $\lesssim 5''$  (Weidinger et al. 2005; Zafar et al. 2011). These  $\text{Ly}\alpha$  photons are most likely radiated from ambient gas illuminated by their associated quasars (Weidinger et al. 2004). On the other hand, DLAs in proximity to quasars with  $z_{\text{abs}} \approx z_{\text{em}}$  proximate damped  $\text{Ly}\alpha$  absorptions (PDLAs; Prochaska et al. 2008) appear to preferentially exhibit residual  $\text{Ly}\alpha$  emission in their absorption troughs (e.g., Møller & Warren 1993; Møller et al. 1998; Ellison et al. 2002; Hennawi et al. 2009; Finley et al. 2013; Fathivavsari et al. 2015). Similar to  $\text{Ly}\alpha$  “blobs,” fluorescent recombination radiation from ambient gas photo-ionized by the quasar, rather than star formation activity in the quasar host galaxy, is likely the main contributor to the residual  $\text{Ly}\alpha$  emission found in PDLAs. This is the case for the strong  $\text{Ly}\alpha$  emission ( $L_{\text{Ly}\alpha} = 3.9 \times 10^{43} \text{ erg s}^{-1}$ ) superposed on the trough of the PDLA toward the quasar SDSS J124020.91+145535.6 (hereafter J1240+1455;  $z = 3$ ; Hennawi et al. 2009). The residual  $\text{Ly}\alpha$  emission is resolved by long-slit spectroscopy to be an  $\text{Ly}\alpha$  blob with spatial extent exceeding  $5''$  around the quasar (e.g., Christensen et al. 2006; Hennawi et al. 2009). Finley et al. (2013) identified 26 PDLAs showing residual narrow  $\text{Ly}\alpha$  emissions with strengths similar to that of the  $\text{Ly}\alpha$  emission observed in J1240-1455 from DR9 and DR10.

<sup>6</sup> SDSS: Sloan Digital Sky Survey; BOSS: Baryon Oscillation Spectroscopic Survey.

In the course of a survey for quasar intermediate-width emission lines (IELs; Li et al. 2015) in SDSS DR12,<sup>7</sup> we found a high-confidence Ly $\alpha$  IEL candidate in the spectrum of the quasar SDSS J095253.83+011422.0 (hereafter J0952+0114) at  $z = 3.020$ . The observed Ly $\alpha$  line is extremely narrow (FWHM  $\sim 1000 \text{ km s}^{-1}$ ) in comparison with the broad metal emission lines (FWHM  $\sim 9000 \text{ km s}^{-1}$ ). The absence of a broad Ly $\alpha$  emission line in J0952+0114 was first reported by Hall et al. (2004) using the SDSS-I/II spectrum. The authors suggested that the broad line region might be dominated by very dense gas ( $10^{15} \text{ cm}^{-3}$ ) in which broad Ly $\alpha$  emission is suppressed, but unusual ionization parameters and peculiar configuration of the emitting clouds are required to reproduce the emission line spectrum. An alternative explanation, that the broad Ly $\alpha$  emission is removed by smooth absorption arising from N v and Ly $\alpha$ , was also discussed, but regarded as unlikely (Hall et al. 2004).

The BOSS spectra of J0952+0114, covering a wider wavelength range than the SDSS spectrum, provide a new insight into this exotic quasar. The damped Ly $\beta$  absorption, the high-order Lyman-series absorptions, and the Lyman limit absorption edge at  $z_{\text{abs}} \approx z_{\text{em}}$  are firmly detected at the blue end of its two BOSS spectra. These detections demonstrate that a high column density PDLA intercepts the sightline to the quasar. The damped Ly $\alpha$  absorption trough removes the intrinsic broad Ly $\alpha$  emission of the quasar completely. The observed narrow Ly $\alpha$  emission line should arise from the ambient gas in an extended area, which is larger than the cross-section of the PDLA cloud. The geometry of this system (i.e., the background quasar, the PDLA cloud, and the emitting gas) is similar to that of the system seen toward the quasar J1240+1455 (Hennawi et al. 2009). However, the luminosity of the residual Ly $\alpha$  emission observed in J0952+0114 is much larger than that in SDSS J1240+1455, by nearly two orders of magnitude, plausibly indicating that they have different origins.

This paper is organized as follows. In Section 2, we summarize the observations. Detailed analysis of the absorption and emission spectrum are presented in Section 3. In Section 4, we discuss the origin of the luminous Ly $\alpha$  emission in J0952+0114 as well as applications and implications. We then provide a summary in Section 5. Throughout this paper,  $H_0$  is taken to be  $70.3 \text{ km s}^{-1} \text{ Mpc}^{-1}$ ,  $\Omega_m = 0.27$ , and  $\Omega_\Lambda = 0.73$ .

## 2. OBSERVATIONS

J0952+0114 is a quasar at  $z = 3.020$  identified by SDSS. Two spectra were first acquired with the SDSS spectrograph (York et al. 2000) fed with fibers in diameters of  $3''$  on 2000 March 05 and December 30. The spectra spread over a wavelength range of  $\lambda \sim 3800\text{--}9200 \text{ \AA}$ . Two additional spectra were taken using the BOSS spectrograph (Dawson et al. 2013), which are fed with  $2''$  fibers and provide a more extended wavelength coverage of  $\lambda \sim 3600\text{--}10400 \text{ \AA}$ , on 2010 December 09 and 2011 March 25. All of the spectra share a similar spectral resolution of  $R \sim 2000$ . We carefully compared the SDSS spectra with the BOSS spectra in continuum, emission lines, and absorption lines. No significant variation in either of these spectral features spanning  $\sim 2$  years in the quasar's rest-frame is detected. Figure 1 presents the combined BOSS spectrum of J0952+0114.<sup>8</sup> The Ly $\alpha$  emission

line is significantly narrower than the broad metal emission lines (see inserted panel in Figure 1). Moreover, an associated C IV absorption system with plenty of absorption lines is identified at  $z_{\text{abs}} = 3.010$ .

## 3. DATA ANALYSIS AND RESULTS

### 3.1. Identification of PDLA

The BOSS spectrum of J0952+0114 ranges from 895 to 2550  $\text{\AA}$  in the quasar's rest-frame. It enables us to search for the neutral hydrogen Lyman-series absorptions corresponding to the associated C IV absorber (Figure 2(a)). First, the damped absorption trough of Ly $\beta$  is credibly identified, which is much broader than any other obvious absorption features (possibly intervening Ly $\alpha$  absorption lines) blanketing the spectrum at  $\lambda < 1216 \text{ \AA}$ . The higher-order Lyman-series absorption, from Ly $\gamma$  to even Ly9, can be identified despite contamination from the Ly $\alpha$  forest. In the very blue end of the spectrum, the flux at rest wavelengths  $\lambda < 912 \text{ \AA}$  is deeply suppressed, suggesting an optically thick neutral hydrogen cloud at the Lyman limit. All of these facts, especially the presence of the damped Ly $\beta$  absorption, reveal that the associated absorber has a high column density of neutral hydrogen.

In order to normalize the observed spectrum, we model the unabsorbed spectrum of J0952+0114 with the composite *Hubble Space Telescope* (HST) quasar spectrum (Zheng et al. 1997) as an initial guess. The quasar continua fit well with each other, but the observed emission line of Ly $\beta$ +O VI is stronger than that in the composite spectrum (Figure 2(a)). In the composite HST spectrum, the ultraviolet (UV) continuum can be modeled as a broken power law with a spectral index of  $\alpha = -2.2$  at  $350 \text{ \AA} \leq \lambda \leq 1050 \text{ \AA}$  ( $f_\nu \propto \nu^\alpha$ ) and  $\alpha = -0.99$  at  $1050 \text{ \AA} \leq \lambda \leq 2200 \text{ \AA}$  (Zheng et al. 1997). We model the UV continuum of J0952+0114 using the same broken power law and model the Ly $\beta$ +O VI emission line with one broad Gaussian. The full model of the unabsorbed spectrum is presented in Figure 2(a) and is applied for normalization.

We measure the column density of neutral hydrogen using Voigt profile fitting to the Ly $\beta$  trough (Figure 2(b)). The best-fit model well reproduces the damped wings of Ly $\beta$ , while there is very weak residual flux in the line center. We infer that the residual flux is the Ly $\beta$  emission associated with the strong Ly $\alpha$  emission of interest. The Voigt profile fitting results in a column density of  $\log N_{\text{H I}} (\text{cm}^{-2}) = 21.8 \pm 0.1$ . Considering the systematic error due to the uncertainty of normalization, we conservatively increase the error by 0.1 dex and adopt  $\log N_{\text{H I}} (\text{cm}^{-2}) = 21.8 \pm 0.2$ . We have demonstrated that the associated absorber toward J0952+0114 is a very strong PDLA. Any Ly $\alpha$  emission from the regions covered by the PDLA cloud in the line of sight should be completely blocked. The observed Ly $\alpha$  emission in J0952+0114 necessarily arises from extended regions around the quasar nucleus (or in the host galaxy), which is beyond the coverage of the PDLA cloud.

Jenkins (1990) proposed a technique to deduce the velocity dispersion of absorbers from the convergence of the Lyman-series lines at wavelengths just above the Lyman limit. The Lyman line convergence technique is very useful for low-resolution spectra (Hurwitz & Bowyer 1995). However, the Lyman edge cannot be confidently identified in the spectrum of J0952+0114, due to heavy contamination from Ly $\alpha$  forest absorption and the relatively low signal-to-noise ratio of data in this spectral region. Instead, we estimate the Doppler

<sup>7</sup> <http://www.sdss.org/dr12/>

<sup>8</sup> The dust map of Schlafly & Finkbeiner (2011) is implemented to correct for Galactic extinction.

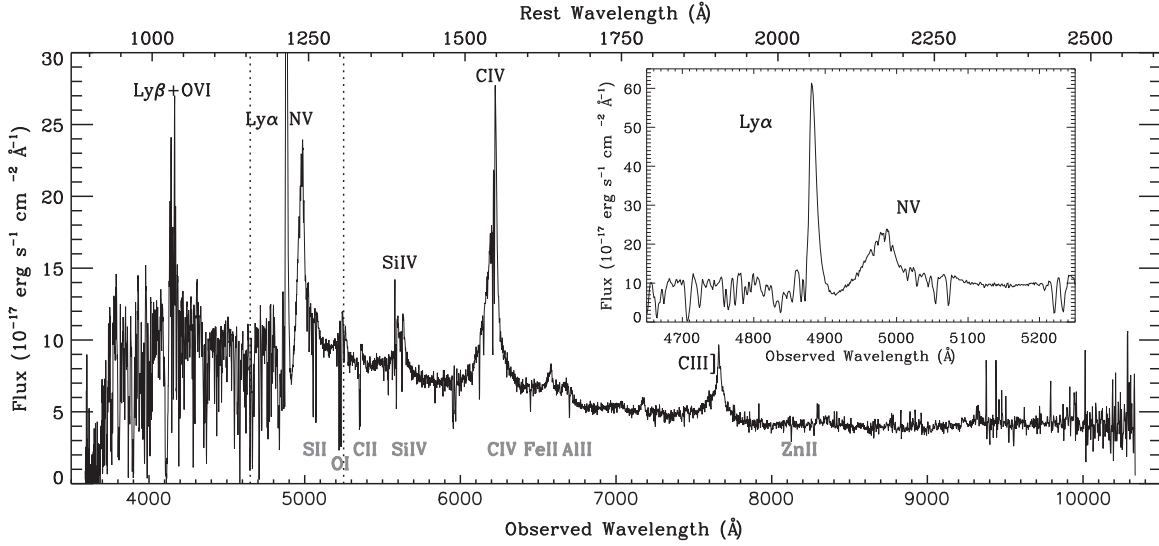


**Figure 1.** Combined BOSS spectrum of J0952+0114. If not stated specifically, the rest wavelength in all figures of this paper corresponds to the rest-frame of the quasar at  $z = 3.020$ . The emission lines and the strong absorption lines are labeled with dark and light characters, respectively. The inserted panel zooms in on the Ly $\alpha$  and N v region indicated by the two vertical dotted lines.

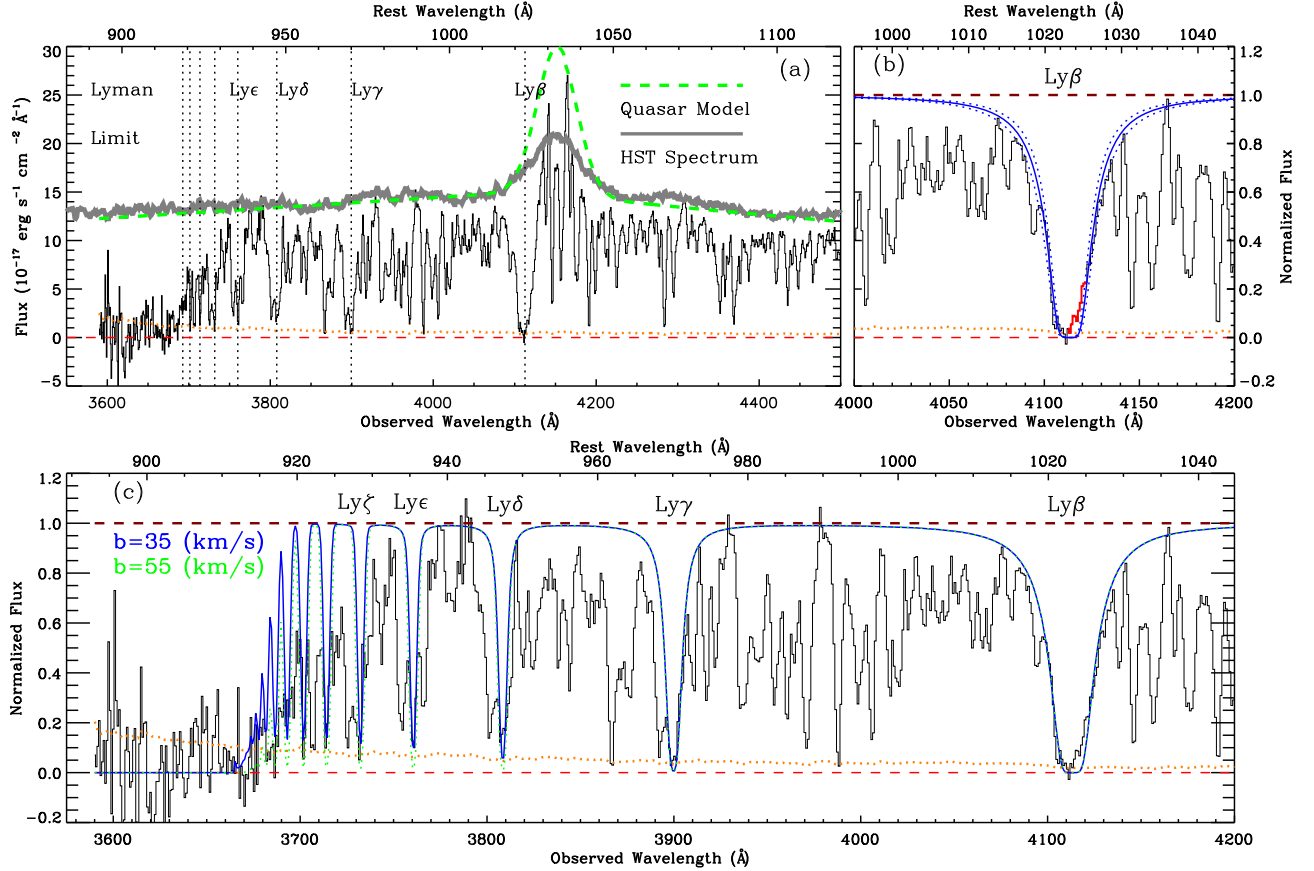


**Figure 2.** Analysis of Lyman-series absorption in the spectrum of J0952+0114. (a) Normalization of the spectrum: the thick gray curve is the composite *HST* quasar spectrum, the dashed green curve is the model of quasar emission constituted by a broken power law and a Gaussian. (b) Voigt profile fitting to the damped Ly $\beta$  trough:  $N_{\text{H I}} = 10^{21.8 \pm 0.2} \text{ cm}^{-2}$ , the residual flux in the line center is labeled in red. (c) Modeling of the Lyman-series absorption and the Lyman limit: the solid blue curve is the model with  $N_{\text{H I}} = 10^{21.8} \text{ cm}^{-2}$  and  $b = 35 \text{ km s}^{-1}$ ; the dotted green curve is the model with  $N_{\text{H I}} = 10^{21.8} \text{ cm}^{-2}$  and  $b = 55 \text{ km s}^{-1}$ , having zero fluxes at the line centers of the Lyman-series absorption. The dotted orange curve is the flux noise in the spectrum.

parameter  $b$  by fitting the depths of high-order Lyman-series lines. With such a high neutral hydrogen column density of  $\log N_{\text{H I}}(\text{cm}^{-2}) \sim 21.8$ , the Lyman-series absorption lines, in orders up to Ly9, should be saturated. The non-zero fluxes

observed at the positions of the line centers (Figure 2(c)) indicate that the lines are not resolved. If the instrumental resolution is given, then we can express the line depths solely as functions of  $b$ . Adopting the derived  $N_{\text{H I}}$  and the spectral

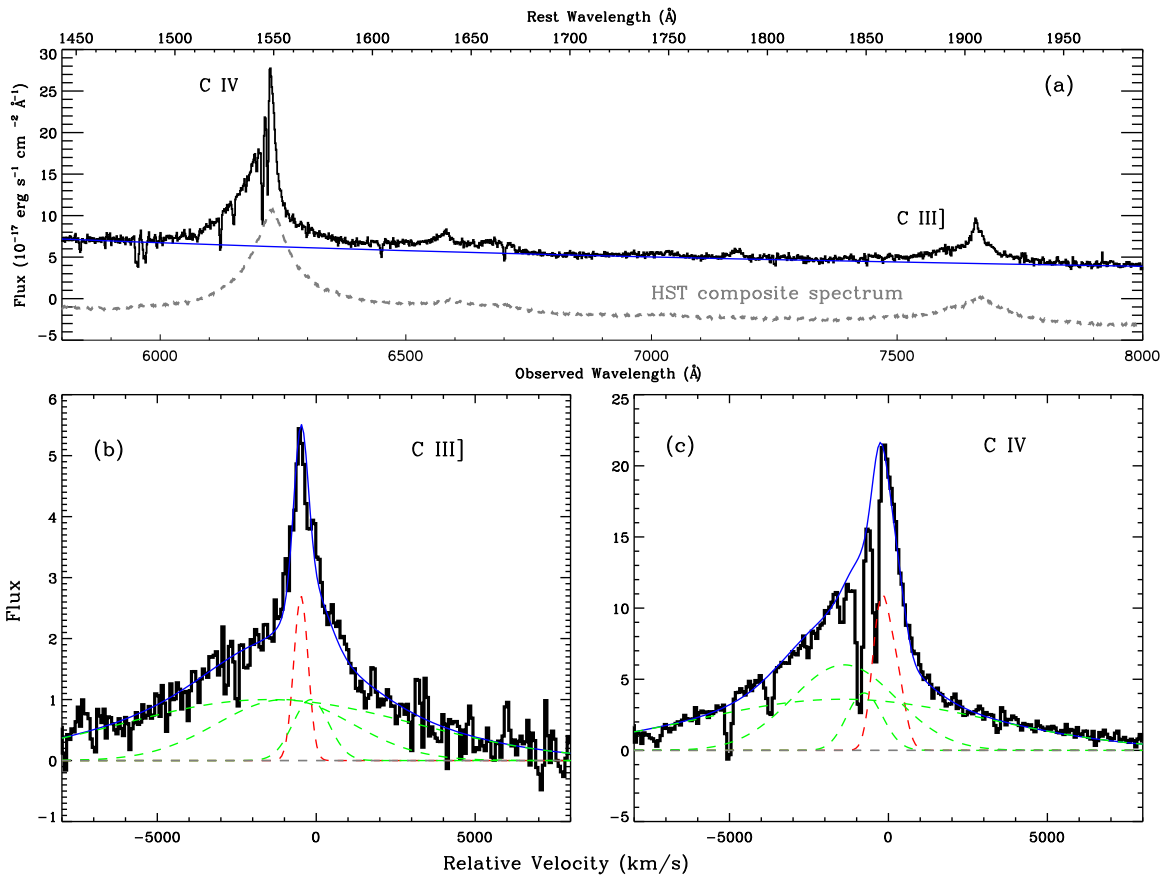


**Figure 3.** Decomposition of C III] and C IV emission lines. (a) Comparison of J0952+0114’s spectrum to the composite *HST* quasar spectrum (shifted vertically for illustration purpose). The continuum is fitted with a power law (in blue) and then subtracted from the spectrum. (b) Decomposition of C III] emission line with four Gaussians; the narrow component is in red. (c) Decomposition of C IV emission line.

dispersion function provided along with the BOSS spectra, we vary  $b$  to fit the observed depths of Lyman-series absorption lines. A best-fit model with  $b = 35 \text{ km s}^{-1}$  is derived, and a minimum width of  $b = 55 \text{ km s}^{-1}$  is found for the models having zero fluxes at the centers of the Lyman series up to Ly9, which appears to disagree with the observation. Since the high-order Lyman-series lines are seriously contaminated by the Ly $\alpha$  absorption forest, it is difficult to gauge the uncertainty of  $b$ . We conservatively adopt the fairly loose upper limit of  $b < 55 \text{ km s}^{-1}$  in the following analysis.

### 3.2. C III] and C IV Emission Lines

The C III] and C IV lines are the strongest broad emission lines in the BOSS spectrum of J0952+0114 (Figure 3(a)). The narrow C IV and C III] emission lines are strong when compared to the composite *HST* quasar spectrum. The line profiles of C IV and C III] are obtained by subtracting a power-law continuum from the observed spectrum, presented in velocity space in Figures 3(b) and (c), respectively. We fit the line profile of C III] with four Gaussians (Figure 3(b)). Three Gaussians are used to model the complex profile of the broad component and the other one for the narrow component. The narrow C III] emission line is so prominent that it is fairly well constrained, yielding  $\text{FWHM} = 532 \pm 37 \text{ km s}^{-1}$ . Since the associated C IV absorption lines are extremely narrow, the line profile of C IV emission is mostly preserved. We directly mask the absorption trough and fit the remaining profile also using four Gaussians (Figure 3(c)). A strong narrow C IV emission line with

$\text{FWHM} = 631 \pm 48 \text{ km s}^{-1}$  is firmly detected. As a brief summary, both of the C III] and C IV emission lines of J0952+0114 are decomposed into a complex broad component arising from the broad emission line region (BELR) and a narrow Gaussian component arising from the narrow emission line region (NELR).

Furthermore, the coverage of the PDLA to NELR, the outermost region of the quasar J0952+0114’s nucleus, is investigated by analyzing the line ratios of the isolated C IV absorptions in different cases. Assuming that the absorber fully covers the nucleus, we divide the observed spectrum by the full model of quasar emission in the C IV region to normalize the C IV absorption lines. The normalized spectrum is presented in Figure 4(a). The rest-frame equivalent widths (EWs) are  $\text{EW}(\text{C IV } \lambda 1548) = 0.69 \pm 0.03 \text{ \AA}$  and  $\text{EW}(\text{C IV } \lambda 1550) = 0.60 \pm 0.03 \text{ \AA}$ , respectively. If the absorber does not cover the NELR, then the narrow C IV emission line should be subtracted before normalization. This yields  $\text{EW}(\text{C IV } \lambda 1548) = 0.71 \pm 0.03 \text{ \AA}$  and  $\text{EW}(\text{C IV } \lambda 1550) = 0.88 \pm 0.03 \text{ \AA}$  (Figure 4(b)). The oscillator strength of C IV  $\lambda 1548$  is twice as large as that of C IV  $\lambda 1550$ , and thus their equivalent width ratio should range from 2 (both of the absorption lines are in the linear part of the curve of growth) to nearly 1 (doublets are seriously saturated). In theory, the line ratio of C IV  $\lambda 1548$  and C IV  $\lambda 1550$  must be no less than one. The second scenario, providing an unpractical line ratio, is therefore ruled out. The analysis indicates that the quasar nucleus of J0952+0114 is fully covered by the associated absorber (i.e., the PDLA).

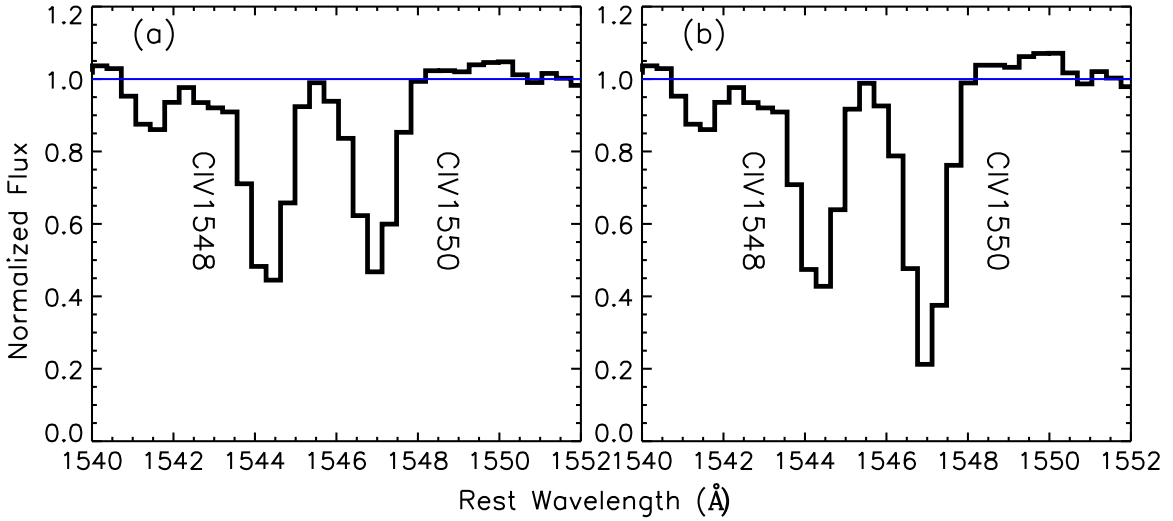


**Figure 4.** Coverage analysis of the associated C IV absorption lines. (a) The absorption lines are normalized assuming that the absorber fully covers the quasar nucleus. (b) The absorption lines are normalized assuming that the absorber does not cover the quasar NELR.

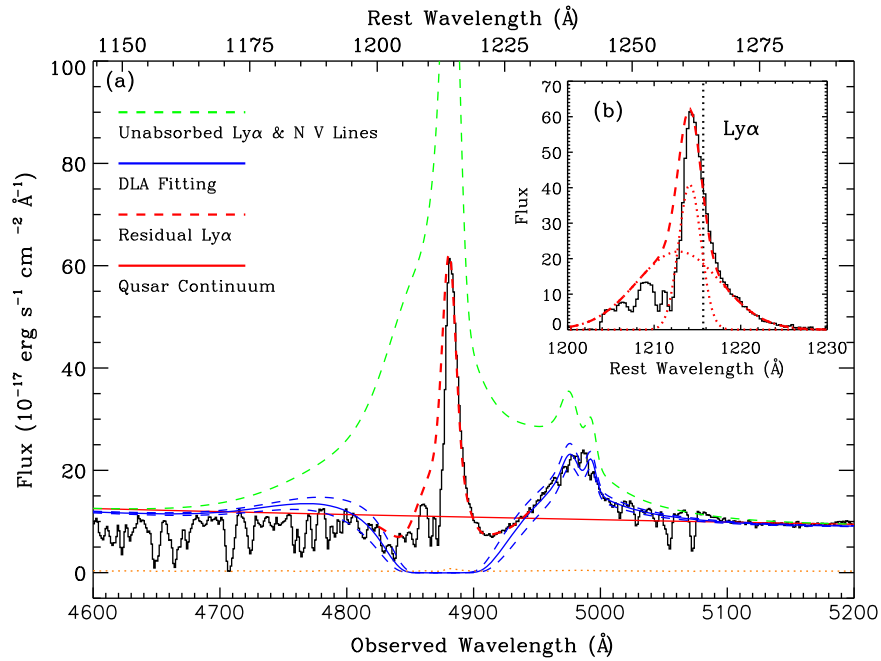


**Figure 5.** (a) Fitting the DLA profile with the column density of  $N_{\text{H I}} = 10^{21.8 \pm 0.2} \text{ cm}^{-2}$ . The unabsorbed quasar emission consists of a power-law continuum and the broad Ly $\alpha$  and N v emission lines, which are modeled with the C IV emission profile; (b) the residual Ly $\alpha$  emission is obtained by subtracting the best-fit DLA model from the observed spectrum. It is then fitted with two Gaussians to correct for the absorption from the Ly $\alpha$  forest.

### 3.3. The Residual Ly $\alpha$ Emission

In our scenario, the spectrum of J0952+0114 in the Ly $\alpha$  band is the sum of the absorbed quasar emission, by the PDLA, and the residual Ly $\alpha$  emission superposed on the absorption trough. The column density  $N_{\text{H I}}$  of the PDLA has been obtained by fitting the associated Ly $\beta$  damped trough. To model the absorbed quasar emission, we have to reconstruct the intrinsic quasar emission, which consists of a continuum and intrinsic Ly $\alpha$  and N v emission lines. The quasar continuum can be well modeled by a power law in a wide wavelength range (Figure 5(a)). However, the flux on both sides of the Ly $\alpha$  emission is significantly lower than the model continuum. The suppressed flux can be naturally explained as the damped wings of the associated Ly $\alpha$  absorption. Assuming the intrinsic

Ly $\alpha$  and N v emission lines share the line profile of C IV emission, we utilize the best-fit profile of the C IV line to model them. The intrinsic quasar emission is then absorbed by the PDLA with a fixed column density of  $\log N_{\text{H I}}(\text{cm}^{-2}) = 21.8$ . We adjust the strengths of the model emission lines to fit the partially observed damped wings of PDLA. The residual Ly $\alpha$  emission is finally derived by subtracting the best-fit model of the absorbed quasar spectrum from the observed spectrum (Figure 5(b)).

The blue wing of the residual Ly $\alpha$  emission is destroyed by the Ly $\alpha$  forest absorption. In order to repair its profile, we model the Ly $\alpha$  emission with two Gaussians by requiring the model to fit the red wing and predict a blue wing to match the imperfect envelope. The width of the repaired Ly $\alpha$  line is  $\text{FWHM} = 1106 \pm 75 \text{ km s}^{-1}$ . The total flux of the residual

$\text{Ly}\alpha$  emission is  $f = 1.64 \pm 0.08 \times 10^{-14} \text{ erg s}^{-1} \text{ cm}^{-2}$ , yielding a luminosity of  $L_{\text{Ly}\alpha} = 1.36 \pm 0.06 \times 10^{45} \text{ erg s}^{-1}$ . The directly integrated residual line flux is also calculated, which is  $f = 1.23 \times 10^{-14} \text{ erg s}^{-1} \text{ cm}^{-2}$ , and the corresponding luminosity is  $L_{\text{Ly}\alpha} = 1.02 \times 10^{45} \text{ erg s}^{-1}$ .

### 3.4. Associated Absorption Lines of Heavy Elements

The associated absorber at  $z_{\text{abs}} = 3.010$  imprints plenty of metal absorption lines in the spectrum of J0952+0114. The absorption lines in the featureless continuum are normalized in a straightforward manner: dividing the observed spectrum by a power law fitted to the local continuum. For the absorption lines superposed on emission lines, we first fit the emission profiles with one to four Gaussians and then divide the observed spectrum by the best-fit model.

$\text{Zn II}\lambda\lambda 2026, 2062$  absorption lines are detected in the BOSS spectrum. However, these two absorption lines may be blended with the  $\text{Mg I}\lambda 2026$  and  $\text{Cr II}\lambda 2062$  lines, respectively. A search for the stronger  $\text{Cr II}\lambda 2056$  line associated with  $\text{Cr II}\lambda 2062$  results in a non-detection, suggesting that  $\text{Zn II}\lambda 2062$  absorption is almost isolated. Therefore, the detections of the  $\text{Zn II}\lambda 2062$  line and the corresponding stronger  $\text{Zn II}\lambda 2026$  line are solid. Highly ionized absorption lines and lines from excited fine-structure levels are useful diagnostics for the physical parameters of quasar absorbers (Ellison et al. 2010).  $\text{N V}\lambda\lambda 1238, 1242$  absorption lines are clearly detected in the spectrum. Three lines of  $\text{Si II}^*$  (i.e.,  $\text{Si II}^*\lambda 1264, \text{Si II}^*\lambda 1309, \text{and Si II}^*\lambda 1533$ ) are tentatively detected, but  $\text{Si II}^*\lambda 1264$  and  $\text{Si II}^*\lambda 1533$  lines are then identified to be an intervening  $\text{Fe II}\lambda 2382$  absorption line at  $z = 1.13$  and a  $\text{C IV}\lambda 1548$  absorption line at  $z = 2.97$ . The isolated absorption line of  $\text{Si II}^*\lambda 1309$  looks strong but its profile is too much broader than that of other metal lines. We conclude that all of the detections of  $\text{Si II}^*$  transitions are false positives. The  $\text{O I}^*\lambda 1304$  absorption line is detected, but it is seriously blended with  $\text{Si II}\lambda 1304$  and  $\text{O I}^*\lambda 1306$  lines (Figure 6). None of the absorption lines from excited states of  $\text{Fe}^+$  are detected in the BOSS spectrum of J0952+0114. We illustrate several absorption lines in Figure 6.

EWs of the absorption lines are measured by integrating the normalized spectrum over a velocity range of  $[-400, 400] \text{ km s}^{-1}$ . The results are summarized in Table 1. In Section 3.1, we obtained the upper limit of the Doppler parameter (i.e.,  $b < 55 \text{ km s}^{-1}$ ). In Figure 7, we present four curves of growth (COG; Jenkins 1986) with Doppler parameters of  $b = 55 \text{ km s}^{-1}, b = 35 \text{ km s}^{-1}, b = 25 \text{ km s}^{-1}, \text{ and } b = 15 \text{ km s}^{-1}$ , respectively.

We can see that the shape of the COG changes dramatically with  $b$ . COGs with smaller Doppler parameters have narrower linear parts. Thus, reducing the value of  $b$  gradually from  $55 \text{ km s}^{-1}$  to  $15 \text{ km s}^{-1}$  will cause most of the detected absorption lines to move into of the logarithmic part where the column density is highly sensitive to both  $b$  and EWs. Reliable column density measurements using the metal absorption lines detected in J0952+0114 therefore cannot be achieved, given that the Doppler parameter cannot be determined in advance (Prochaska 2006). We locate the metal absorption lines on the COG of  $b = 55 \text{ km s}^{-1}$ . The column densities measured on it are therefore conservative lower limits. In this manner, we estimate the column density of zinc, yielding  $N_{\text{Zn}^+} > 10^{13.4} \text{ cm}^{-2}$ . The relative abundance to the solar value is  $[\text{Zn}/\text{H}] > -1.0$ , i.e., in the range of metal-strong

DLAs (e.g., Kaplan et al. 2010; Wang et al. 2012). It is worth following up on the PDLA toward J0952+0114 using high-resolution spectroscopy to measure the column densities more precisely.

## 4. DISCUSSION

### 4.1. PDLA Cloud

In J0952+0114, the requirement of proximity to a hard ionizing source for the presence of  $\text{N V}$  transitions, which are rarely seen in intervening DLAs, constrains the distance between the quasar and absorber to be  $d < 1 \text{ Mpc}$  (Fox et al. 2009; Hennawi et al. 2009). Ellison et al. (2010) studied seven PDLA systems with high-resolution spectroscopy and estimated a lower limit for the distance  $d > 150 \text{ kpc}$  via the UV pumping rate estimated by the strengths of  $\text{Si II}^*$  absorption. Thus, those PDLAs are unlikely to be associated with their quasar hosts, but rather foreground galaxies in proximity to the quasar. Recently, Fathivavsari et al. (2015) reported an intrinsic DLA toward the quasar SDSS J082303.22+052907.6. The distance of the absorbing cloud to the quasar nucleus is  $d < 1 \text{ kpc}$ , and extended  $\text{Ly}\alpha$  emission was observed with the assistance from the coronagraphic cloud. However, the origin of the PDLA toward J0952+0114 can hardly be determined in this way, as the  $\text{Si II}^*$  transitions are not detected in the spectrum.

The coverage analysis of the  $\text{C IV}$  absorption lines has revealed that the PDLA cloud is on a scale larger than the NELR of J0952+0114. If the PDLA absorber is the interstellar medium (ISM) in the quasar host galaxy or in a foreground galaxy, then its volume density might be similar to regular DLAs, in the range of  $n_{\text{H}} \sim 1\text{--}100 \text{ cm}^{-3}$  (Prochaska & Hennawi 2009). Assuming a homogeneous density in the cloud, we estimate its length scale to be  $r = N_{\text{H}}/n_{\text{H}} \approx 20 \text{ pc--}2 \text{ kpc}$ . It is consistent with, and more extended in a way, than the scales of the NELR observed in local active galactic nuclei (AGNs; e.g., Kraemer et al. 1994; Hutchings et al. 1998; Peterson et al. 2013). If the PDLA cloud has a higher density, then it would necessarily be closer to the quasar nucleus, more likely in the quasar host galaxy, to maintain a relatively high ionization parameter  $U$  to produce  $\text{N V}$  absorption lines. Ji et al. (2015) identified an intrinsic absorber, via its  $\text{He I}^*$  and  $\text{Fe II}^*$  absorption lines, toward the quasar SDSS J080248.18+551328.9 and derived a density of  $n_{\text{H}} \sim 10^5 \text{ cm}^{-3}$ , a distance of 100–250 pc to the nucleus. The PDLA of interest is unlikely to have such a high density, otherwise the corresponding size will be too small to cover the quasar NELR in that case.

### 4.2. Origin of the Luminous $\text{Ly}\alpha$ Emission

The quasar J0952+0114 was initially selected as an IEL quasar candidate. However, the  $\text{Ly}\alpha$  IEL scenario has to be ruled out. As the NELR, i.e., the outermost region of quasar nucleus, is already covered by the PDLA cloud, the IEL region that presumably exists between the BELR and NELR (e.g., Brotherton et al. 1994) must be blocked in the  $\text{Ly}\alpha$  band.

Outflows over NELR scales have been observed widely, traced by the optical emission lines of their photoionized gas, in nearby AGNs (e.g., Fu & Stockton 2009; Liu et al. 2013; Harrison et al. 2014). The emission lines arising from those outflows generally have velocity widths of  $\sim 800 \text{ km s}^{-1}$ , which are above the escape velocities from the host galaxies. Having a similar line width, the  $\text{Ly}\alpha$  emission of J0952+0114 is very

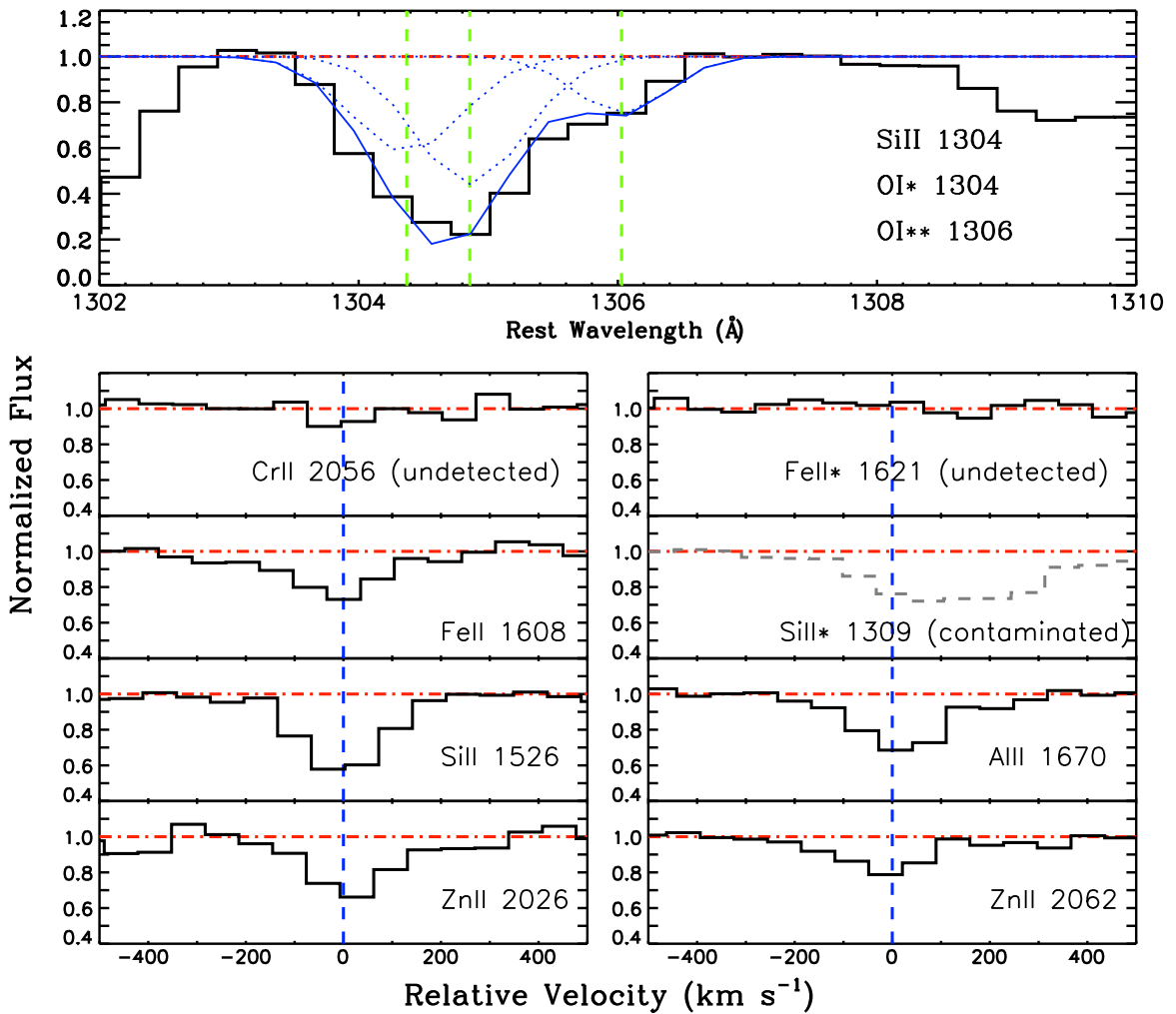


**Figure 6.** Associated absorptions lines of interest in J0952+0114. The blended absorption profile (solid blue curve) around  $\lambda_{\text{rest}} = 1305 \text{ \AA}$  is demonstrated at the absorber’s rest-frame at  $z = 3.010$ . It is decomposed into three Gaussians (thin dotted curves): Si  $\pi\lambda 1304$ , O  $\text{I}^*\lambda 1304$ , and O  $\text{I}^{**}\lambda 1306$  with their line centroids marked by green dashed lines from left to right. In the other panels, zero velocities (blue dashed lines) correspond to a redshift of  $z = 3.010$ .

likely fluorescent recombination radiation from outflows driven by the quasar. We derive a covering factor of the emitting gas as  $cf = L_{\text{Ly}\alpha}/(0.6h\nu)/Q = 9\%$ , where the ionizing photon rate  $Q \sim 1.1 \times 10^{57} \text{ s}^{-1}$  is estimated by scaling the observed spectrum with the MF87 spectral energy distribution (SED; Mathews & Ferland 1987) and case B recombination is assumed. This is over an order of magnitude larger than that of the Ly $\alpha$  blobs observed around quasars ( $cf \approx 0.5\%$ ; e.g., Heckman et al. 1991; Christensen et al. 2006). The large covering factor also supports the outflow scenario rather than quiescent ISM or infalling gas into/onto the quasar host galaxy (Rees 1988; Haiman & Rees 2001; Hennawi et al. 2009).

The spatial extent of outflows is critical to the evaluation of whether or not a quasar is able to input its energy effectively into the ISM of its host galaxy. Only galaxy-scale outflows are efficient quasar feedbacks, which can quench star formation widely in quasar hosts and therefore regulate the evolution of galaxies (e.g., Silk & Rees 1998; Di Matteo et al. 2005). Meanwhile, the discovery of a significant population of massive evolved galaxies at  $z > 1.5$  (e.g., McCarthy et al. 2004; Saracco et al. 2005) requires that quasar feedback must have impinged in the early universe. Observations of galaxy-scale outflows are desired to study the quasar feedback

at high redshifts. However, it is challenging to identify the extended outflows from the “seeing fuzz” of bright quasars, even if they are large enough to be spatially resolved. Currently, most high-redshift galaxy-scale outflows serving as evidence for quasar feedback in the early universe are actually observed in radio galaxies and ultraluminous infrared galaxies (e.g., Nesvadba et al. 2008; Alexander et al. 2010; Harrison et al. 2012) where the central AGNs are obscured and/or intrinsically dim. With the assistance of a PDLA blocking the emission at Ly $\alpha$  wavelengths from the background quasars, the galaxy-scale outflows emitting substantial Ly $\alpha$  photons can be easily resolved, using narrow-band imaging and long-slit/integral field spectroscopy, for high-redshift quasars in the bright phase. The successful application of this technique in resolving the weak Ly $\alpha$  “blob” detected in the PDLA trough of the quasar Q0151+048 (Zafar et al. 2011) gives us further confidence in revealing outflows in J0952+0114 analogs.

We then carefully re-examine the SDSS spectra with  $3''$  fiber and the BOSS spectra with  $2''$  fiber, of J0952+0114, to seek for the possible increment of Ly $\alpha$  flux observed in a larger aperture. There is no significant variation in the Ly $\alpha$  line, suggesting that the Ly $\alpha$  emission must be concentrated in  $2''$  on the sky, i.e., a proper size of  $\lesssim 8 \text{ kpc}$  at  $z = 3.020$ . In J0952

**Table 1**  
Metal Absorption Lines of the PDLA

$\lambda_{\text{vacuum}}$ (Å)	Ion	EW (Å)	Note
1238.821	N v	$0.12 \pm 0.03$	...
1242.804	N v	$0.07 \pm 0.02$	...
1250.584	S II	$0.17 \pm 0.02$	...
1253.811	S II	$0.28 \pm 0.02$	...
1259.519	S II	$0.26 \pm 0.02$	...
1260.422	Si II	$0.75 \pm 0.02$	a
1264.737	Si II*	$0.73 \pm 0.02$	a
1302.168	O I	$1.01 \pm 0.02$	...
1304.370	Si II	$0.44 \pm 0.03$	b
1304.857	O I*	$0.58 \pm 0.03$	b
1306.028	O I**	$0.26 \pm 0.03$	b
1309.275	Si II*	$0.51 \pm 0.03$	c
1334.532	C II	$1.22 \pm 0.04$	b
1335.707	C II*	$1.22 \pm 0.04$	b
1393.755	Si IV	$0.49 \pm 0.04$	...
1402.770	Si IV	$0.40 \pm 0.04$	...
1526.706	Si II	$0.46 \pm 0.03$	...
1533.431	Si II*	$0.33 \pm 0.03$	a
1548.195	C IV	$0.69 \pm 0.03$	...
1550.770	C IV	$0.60 \pm 0.03$	...
1608.451	Fe II	$0.36 \pm 0.04$	...
1621.685	Fe II*	$<0.05$	d
1670.787	Al II	$0.41 \pm 0.04$	...
1854.716	Al III	$0.22 \pm 0.04$	...
1862.789	Al III	$0.14 \pm 0.04$	...
2026.136	Zn II	$0.51 \pm 0.06$	...
2056.253	Cr II	$<0.08$	d
2062.664	Zn II	$0.30 \pm 0.06$	...
2344.214	Fe II	$0.43 \pm 0.08$	...

**Note.** Measurements of metal absorption lines in the associated system toward J0952+0114. Error-bars are at the  $1\sigma$  level, including statistical errors and systematic errors due to continuum normalization. (a) Blended with intervening absorption lines at lower redshift. (b) Blended lines. (c) Unknown absorption. (d) Non-detection.

+0114, the luminous Ly $\alpha$  emission contributes  $\sim 8\%$  of the total flux in the SDSS  $g$  band. In Figure 8, we subtract its SDSS image by the point-spread function (PSF) model derived from the nearby stars in the field, which can be fit using a two-dimensional (2D) Gaussian with FWHM =  $1''.3$ . No significant residual flux is detected, and therefore the luminous Ly $\alpha$  emission of interest is not spatially resolved in the SDSS image.

#### 4.3. Applications and Implications

The approach of using DLAs as a natural coronagraph to observe the Ly $\alpha$  emission associated with star formation in their host galaxies has been studied extensively (e.g., Kulkarni et al. 2006; Fynbo et al. 2010; Noterdaeme et al. 2014). The SFR observed in high-redshift Lyman break galaxies (LBGs; Shapley et al. 2003; Erb et al. 2006) and Ly $\alpha$  emitters (LAEs; Cronwall et al. 2007) are  $\sim 30 M_{\odot} \text{ yr}^{-1}$ , while the SFR in quasar host galaxies is  $\sim 9 M_{\odot} \text{ yr}^{-1}$  (e.g., Ho 2005; Cai et al. 2014). Using the Kennicutt (1998) calibration  $\text{SFR}(M_{\odot} \text{ yr}^{-1}) = L(\text{H}\alpha)/1.26 \times 10^{41} \text{ erg s}^{-1}$  and assuming an intensity ratio of Ly $\alpha$ /H $\alpha$  = 8.3 for the case B recombination, we estimate an Ly $\alpha$  luminosity of  $\sim 5 \times 10^{43} \text{ erg s}^{-1}$  for strong star formation activity. This is much lower than the luminosity of the residual Ly $\alpha$  emission observed in J0952

+0114. Conclusively, the residual Ly $\alpha$  emission associated with star formation is fairly weak compared with quasar emission, and thus the DLA troughs can be seen clearly in this case.

The identification of DLA trough becomes difficult if the residual Ly $\alpha$  flux is large enough to fill it almost entirely. It is notable that J0952+0114 was omitted in all of the spectroscopic surveys of DLAs and PDLAs in SDSS (e.g., Prochaska et al. 2008; Noterdaeme et al. 2012b; Finley et al. 2013). More appropriate criteria for selecting J0952+0114 analogs would be as follow: quasars having significantly narrower Ly $\alpha$  emission than their broad C IV lines, jointly with associated damped absorptions from Ly $\beta$  (if its absorption trough is preserved), or associated strong metal absorption lines. Our preliminary survey shows that such systems are not very rare in SDSS quasars. The strong Ly $\alpha$  emission in the candidate systems could be IELs or outflows driven by the quasar, while other explanations are needed for individuals. Follow-up observations with a long-slit, integral field, and high-resolution echelle spectrograph as well as narrow-band imaging will be useful for exploring their natures.

PDLAs, acting like natural coronagraphs, provide us with unique insight into the gaseous content in the vicinity of quasars. Meanwhile, other types of natural coronagraphs exist and are enormously useful for investigations of quasars. Recently, Li et al. (2015) detected a mostly pure Ly $\alpha$  IEL in the quasar OI 287 where the dusty torus, as a natural coronagraph, coincidentally blocks the BELR but leaves the IEL region observable. The unambiguous detection demonstrated the existence of quasar IELs, which has been debated for decades (e.g., Wills et al. 1993; Brotherton et al. 1994; Mason et al. 1996). Strong N v broad absorption line (BAL; e.g., Weymann et al. 1991; Voit et al. 1993; Zhang et al. 2010) absorbers are elegant coronagraphs on the scales of BELRs (Zhang et al. 2015), which are potential tools for exploring the sub-parsec structures in quasars.

## 5. SUMMARY

We revisit the unusual Ly $\alpha$  emission of J0952+0114 (Hall et al. 2004), initially motivated by searching for the quasar IELs (Li et al. 2015). A high column density ( $\log N_{\text{H I}}(\text{cm}^{-2}) = 21.8 \pm 0.2$ ) neutral hydrogen cloud in proximity to the quasar is identified via the detections of an associated damped Ly $\beta$  absorption trough, high-order Lyman-series absorptions, and the Lyman limit absorption edge in the BOSS spectrum of J0952+0114. Meanwhile, the line ratio of the associated C IV absorption suggests that both the BELR and NELR of the quasar are covered by the thick cloud. These new clues merge into a scenario wherein the absence of the broad Ly $\alpha$  line is due to strong PDLA absorption and the residual Ly $\alpha$  emission superposed on the trough is fluorescent recombination radiation from ambient gas outside of the NELR. With a luminosity of  $L_{\text{Ly}\alpha} \sim 10^{45} \text{ erg s}^{-1}$ , the residual Ly $\alpha$  emission is the largest ever seen in either intervening or proximate DLA troughs. The coverage analysis first rules out an IEL origin of the observed Ly $\alpha$  emission. Its relatively broad line width and high luminosity largely exclude the possibility that it is associated with star formation activity, but suggest an origin from outflows driven by a quasar. The proper size of the outflow, inferred from SDSS spectra and images, is  $\lesssim 8$  kpc.

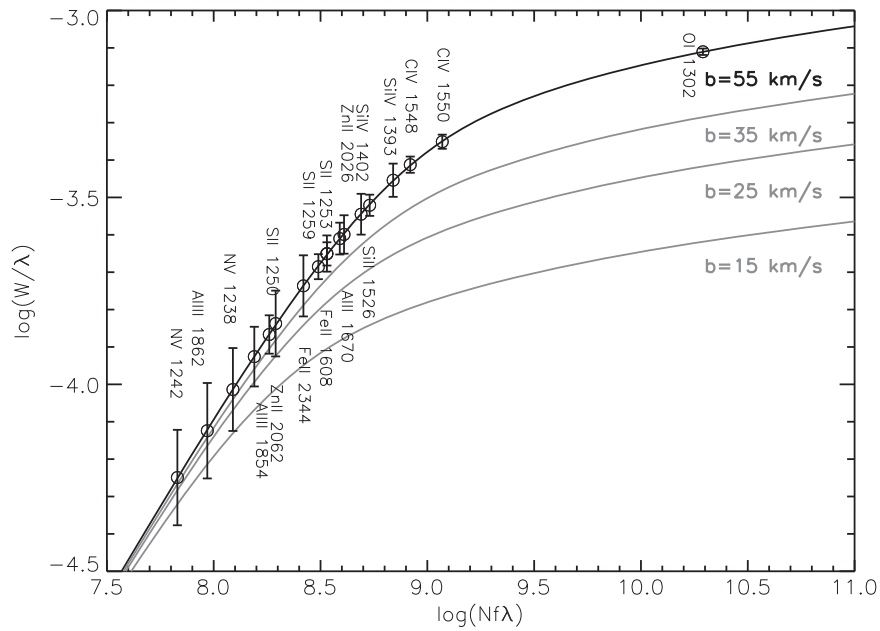


**Figure 7.** Four curves of growth are created with the Doppler parameters  $b = 55 \text{ km s}^{-1}$ ,  $b = 35 \text{ km s}^{-1}$ ,  $b = 25 \text{ km s}^{-1}$ , and  $b = 15 \text{ km s}^{-1}$ , respectively. The associated metal absorption lines are placed onto the curve of  $b = 55 \text{ km s}^{-1}$  in order to estimate the lower limits of their column densities.

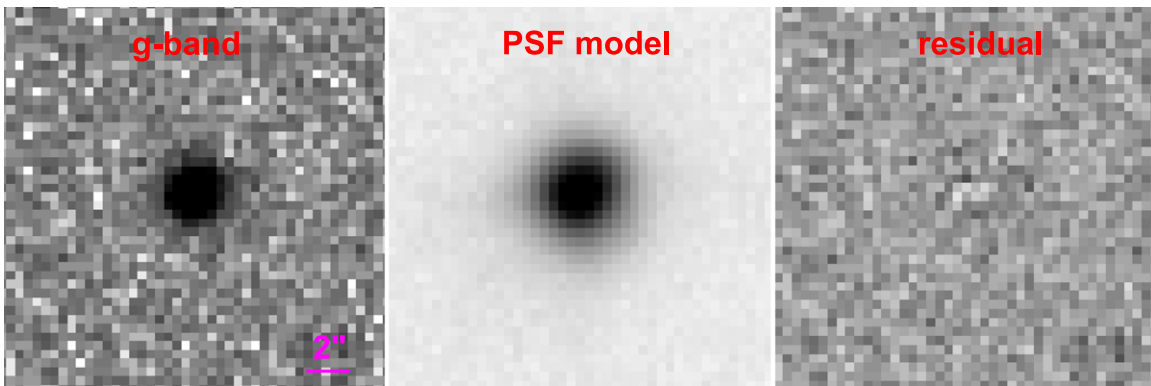


**Figure 8.** SDSS image of J0952+0114 in the  $g$  band is in the left panel; the fitted stellar PSF using a 2D Gaussian with FWHM =  $1''.3$  is in the middle panel. No significant residual flux is detected in the subtracted image (the right panel).

PDLAs, acting like natural coronagraphs, provide us with a good probe into the illuminated gas in the vicinity of quasars, which is hardly resolved due to its small size or “seeing fuzz” of bright quasars. It is worthwhile to search for analogs of J0952+0114 in large-sky spectroscopic surveys, such as SDSS and LAMOST (Zhao et al. 2012). A significantly narrower Ly $\alpha$  emission line than the broad C IV line and an associated damped absorption from Ly $\beta$  are proper criteria for selecting J0952+0114 analogs. Our preliminary survey shows that such systems are not very rare. Follow-up observations with long-slit, integral field, and high-resolution echelle spectrographs, as well as narrow-band imaging, would be useful for exploring the nature of the selected systems. Some of the Ly $\alpha$  emitting gas might be massive galaxy-scale outflows around optically bright high-redshift quasars, which will be direct evidence for the efficient quasar feedback in the early universe which is rarely seen these days.

The authors appreciate the enlightening suggestions from the anonymous referee, which helped to improve the quality of this paper. This work is supported by National Basic Research

Program of China (973 Program, grant No. 2015CB857005, grant No. 2013CB834905), the NSFC grant (grant No. 11233002, 11203022, 11421303, 11473025, 11033007), and the SOC program (CHINARE2015-02-03).

Funding for SDSS-III has been provided by the Alfred P. Sloan Foundation, the Participating Institutions, the National Science Foundation, and the U.S. Department of Energy Office of Science. The SDSS-III web site is <http://www.sdss3.org/>.

SDSS-III is managed by the Astrophysical Research Consortium for the Participating Institutions of the SDSS-III Collaboration including the University of Arizona, the Brazilian Participation Group, Brookhaven National Laboratory, Carnegie Mellon University, University of Florida, the French Participation Group, the German Participation Group, Harvard University, the Instituto de Astrofísica de Canarias, the Michigan State/Notre Dame/JINA Participation Group, Johns Hopkins University, Lawrence Berkeley National Laboratory, Max Planck Institute for Astrophysics, Max Planck Institute for Extraterrestrial Physics, New Mexico State University, New York University, Ohio State University, Pennsylvania State University, University of Portsmouth, Princeton University, the

Spanish Participation Group, University of Tokyo, University of Utah, Vanderbilt University, University of Virginia, University of Washington, and Yale University.

## REFERENCES

- Alexander, D. M., Swinbank, A. M., Smail, I., McDermid, R., & Nesvadba, N. P. H. 2010, *MNRAS*, **402**, 2211
- Brotherton, M. S., Wills, B. J., Francis, P. J., & Steidel, C. C. 1994, *ApJ*, **430**, 495
- Cai, Z., Fan, X., Noterdaeme, P., et al. 2014, *ApJ*, **793**, 139
- Christensen, L., Jahnke, K., Wisotzki, L., & Sánchez, S. F. 2006, *A&A*, **459**, 177
- Dawson, K. S., Schlegel, D. J., Ahn, C. P., et al. 2013, *AJ*, **145**, 10
- Di Matteo, T., Springel, V., & Hernquist, L. 2005, *Natur*, **433**, 604
- Ellison, S. L., Prochaska, J. X., Hennawi, J., et al. 2010, *MNRAS*, **406**, 1435
- Ellison, S. L., Yan, L., Hook, I. M., et al. 2002, *A&A*, **383**, 91
- Erb, D. K., Steidel, C. C., Shapley, A. E., et al. 2006, *ApJ*, **647**, 128
- Fathivavari, H., Petitjean, P., Noterdaeme, P., et al. 2015, *MNRAS*, **454**, 876
- Finley, H., Petitjean, P., Pâris, I., et al. 2013, *A&A*, **558**, A111
- Fox, A. J., Prochaska, J. X., Ledoux, C., et al. 2009, *A&A*, **503**, 731
- Fu, H., & Stockton, A. 2009, *ApJ*, **690**, 953
- Fynbo, J. P. U., Laursen, P., Ledoux, C., et al. 2010, *MNRAS*, **408**, 2128
- Gronwall, C., Ciardullo, R., Hickey, T., et al. 2007, *ApJ*, **667**, 79
- Haiman, Z., & Rees, M. J. 2001, *ApJ*, **556**, 87
- Hall, P. B., Snedden, S. A., Niederste-Ostholt, M., et al. 2004, *AJ*, **128**, 534
- Harrison, C. M., Alexander, D. M., Mullaney, J. R., & Swinbank, A. M. 2014, *MNRAS*, **441**, 3306
- Harrison, C. M., Alexander, D. M., Swinbank, A. M., et al. 2012, *MNRAS*, **426**, 1073
- Heckman, T. M., Lehnert, M. D., Miley, G. K., & van Breugel, W. 1991, *ApJ*, **381**, 373
- Hennawi, J. F., Prochaska, J. X., Kollmeier, J., & Zheng, Z. 2009, *ApJL*, **693**, L49
- Ho, L. C. 2005, *ApJ*, **629**, 680
- Hurwitz, M., & Bowyer, S. 1995, *ApJ*, **446**, 812
- Hutchings, J. B., Crenshaw, D. M., Kaiser, M. E., et al. 1998, *ApJL*, **492**, L115
- Jenkins, E. B. 1986, *ApJ*, **304**, 739
- Jenkins, E. B. 1990, in *The Interstellar Medium in External Galaxies: Summaries of Contributed Papers*, ed. D. J. Hollenbach, & H. A. Thronson (Washington, DC: NASA), 3084
- Ji, T., Zhou, H., Jiang, P., et al. 2015, *ApJ*, **800**, 56
- Kaplan, K. F., Prochaska, J. X., Herbert-Fort, S., Ellison, S. L., & Dessauges-Zavadsky, M. 2010, *PASP*, **122**, 619
- Kennicutt, R. C., Jr. 1998, *ApJ*, **498**, 541
- Kraemer, S. B., Wu, C. C., Crenshaw, D. M., & Harrington, J. P. 1994, *ApJ*, **435**, 171
- Kulkarni, V. P., Meiring, J., Som, D., et al. 2012, *ApJ*, **749**, 176
- Kulkarni, V. P., Woodgate, B. E., York, D. G., et al. 2006, *ApJ*, **636**, 30
- Li, Z., Zhou, H., Hao, L., et al. 2015, *ApJ*, **812**, 99
- Liu, G., Zakamska, N. L., Greene, J. E., Nesvadba, N. P. H., & Liu, X. 2013, *MNRAS*, **436**, 2576
- Mason, K. O., Puchnarewicz, E. M., & Jones, L. R. 1996, *MNRAS*, **283**, L26
- Mathews, W. G., & Ferland, G. J. 1987, *ApJ*, **323**, 456
- McCarthy, P. J., Le Borgne, D., Crampton, D., et al. 2004, *ApJL*, **614**, L9
- Møller, P., Fynbo, J. P. U., & Fall, S. M. 2004, *A&A*, **422**, L33
- Møller, P., & Warren, S. J. 1993, *A&A*, **270**, 43
- Møller, P., Warren, S. J., & Fynbo, J. U. 1998, *A&A*, **330**, 19
- Nagamine, K., Springel, V., & Hernquist, L. 2004, *MNRAS*, **348**, 435
- Nesvadba, N. P. H., Lehnert, M. D., De Breuck, C., Gilbert, A. M., & van Breugel, W. 2008, *A&A*, **491**, 407
- Noterdaeme, P., Laursen, P., Petitjean, P., et al. 2012a, *A&A*, **540**, A63
- Noterdaeme, P., Petitjean, P., Carithers, W. C., et al. 2012b, *A&A*, **547**, L1
- Noterdaeme, P., Petitjean, P., Pâris, I., et al. 2014, *A&A*, **566**, A24
- Peterson, B. M., Denney, K. D., De Rosa, G., et al. 2013, *ApJ*, **779**, 109
- Prochaska, J. X. 2006, *ApJ*, **650**, 272
- Prochaska, J. X., & Hennawi, J. F. 2009, *ApJ*, **690**, 1558
- Prochaska, J. X., Hennawi, J. F., & Herbert-Fort, S. 2008, *ApJ*, **675**, 1002
- Prochaska, J. X., Herbert-Fort, S., & Wolfe, A. M. 2005, *ApJ*, **635**, 123
- Rees, M. J. 1988, *MNRAS*, **231**, 91
- Saracco, P., Longhetti, M., Severgnini, P., et al. 2005, *MNRAS*, **357**, L40
- Schlafly, E. F., & Finkbeiner, D. P. 2011, *ApJ*, **737**, 103
- Shapley, A. E., Steidel, C. C., Pettini, M., & Adelberger, K. L. 2003, *ApJ*, **588**, 65
- Silk, J., & Rees, M. J. 1998, *A&A*, **331**, L1
- Smith, H. E., Cohen, R. D., Burns, J. E., Moore, D. J., & Uchida, B. A. 1989, *ApJ*, **347**, 87
- Voit, G. M., Weymann, R. J., & Korista, K. T. 1993, *ApJ*, **413**, 95
- Wang, J. G., Zhou, H. Y., Ge, J., et al. 2012, *ApJ*, **760**, 42
- Weidinger, M., Møller, P., & Fynbo, J. P. U. 2004, *Natur*, **430**, 999
- Weidinger, M., Møller, P., Fynbo, J. P. U., & Thomsen, B. 2005, *A&A*, **436**, 825
- Weymann, R. J., Morris, S. L., Foltz, C. B., & Hewett, P. C. 1991, *ApJ*, **373**, 23
- Wills, B. J., Netzer, H., Brotherton, M. S., et al. 1993, *ApJ*, **410**, 534
- Wolfe, A. M., Gawiser, E., & Prochaska, J. X. 2005, *ARA&A*, **43**, 861
- Wolfe, A. M., Turnshek, D. A., Smith, H. E., & Cohen, R. D. 1986, *ApJS*, **61**, 249
- York, D. G., Adelman, J., Anderson, J. E., Jr., et al. 2000, *AJ*, **120**, 1579
- Zafar, T., Møller, P., Ledoux, C., et al. 2011, *A&A*, **532**, A51
- Zhang, S. H., Wang, T. G., Wang, H. Y., et al. 2010, *ApJ*, **714**, 367
- Zhang, S. H., Zhou, H. Y., Shi, X. H., et al. 2015, *ApJ*, **815**, 113
- Zhao, G., Zhao, Y. H., Chu, Y. Q., Jing, Y. P., & Deng, L. C. 2012, *RAA*, **12**, 723
- Zheng, W., Kriss, G. A., Telfer, R. C., Grimes, J. P., & Davidsen, A. F. 1997, *ApJ*, **475**, 469